Inorganic Chemistry

Article

pubs.acs.org/IC

[3:1] Site-Differentiated [4Fe−4S] Clusters Having One Carboxylate and Three Thiolates

Tamaki Terada,[†] Kiyohisa Hirabayashi,[†] Dong Liu,[†] Tomohiko Nakamura,[†] Takuya Wakimoto,[†] Tsuyoshi Matsumoto,*[,‡] and Kazuyuki Tatsumi*[,§]

[†]Department of Chemistry, Graduate School of Science, [‡]Institute of Transformative Bio-Molecules (WPI-ITbM), and [§]Research Center for Materials Science, Nagoya University, Furo-cho, Chikusa-ku, Nagoya 464-8602, Japan

Supporting Information

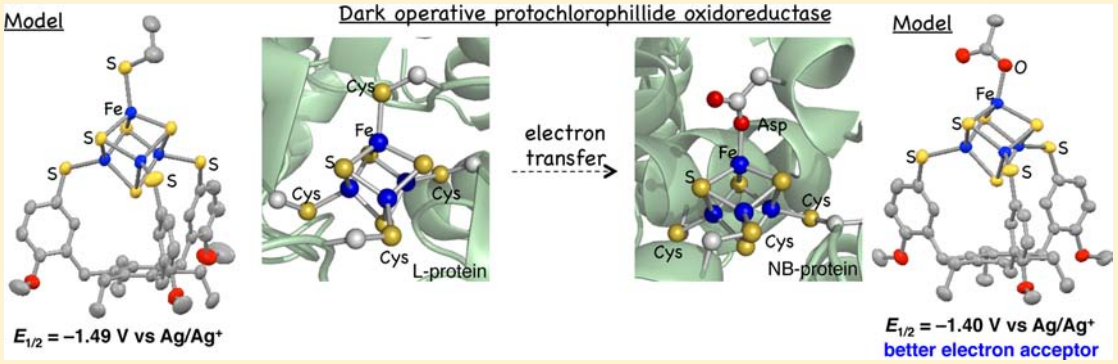

ABSTRACT: [4Fe−4S] clusters modeled after those in organisms having three cysteine thiolates and one carboxylate were synthesized by using the tridentate thiolato chelate. X-ray structural analysis reveals that the carboxylates coordinate to the unique irons in an η^1 manner rather than η^2. Redox potentials show a positive shift from that of the cluster having ethanethiolate and the tridentate thiolato chelate. These properties conform to the arrangement of the [4Fe−4S] clusters in the electron transfer systems included in *Rc* dark operative protochlorophyllide oxidoreductase (DPOR) and formaldehyde oxidoreductase (FOR) with *Pf* ferredoxin.

INTRODUCTION

[4Fe−4S] clusters are essential components in organisms due to their functions in electron transfer, catalytic molecular conversions, and transcriptional regulation.[1] Whereas many of the [4Fe−4S] clusters are coordinated by four cysteine thiolates equally at the four irons, [3:1] site-differentiated [4Fe−4S] clusters carrying one noncysteine ligand have been reported and have attracted much attention.[2−7] Carboxylates are the representative ligand, and those structures included in various proteins have also been demonstrated crystallographically. The aspartate coordination is known in ferredoxin from *Pyrococcus furiosus*[3] and in dark operative protochlorophyllide oxidoreductase (DPOR) from *Rhodobacter capsulatus*,[4] and those clusters function as electron transfer mediators. Aconitase, catalyzing isomerization of citrate into isocitrate,[5] also contains a cluster of this type, and the structure with a unique iron coordinated by isocitrate was analyzed. Similar carboxylate coordination is also reported for the isoprenoid biosynthesis protein (IspG) from *Aquifex aeolicus*,[6] and for radical-SAM superfamily enzymes such as biotin synthase and pyruvate formate-lyase, in which the clusters are chelated by S-adenosylmethionine (SAM) at the carboxylate and the amines have been elucidated (Chart 1).[7]

Chart 1

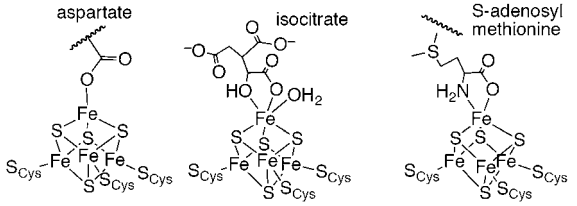

On the other hand, synthetic [4Fe−4S] clusters having both carboxylate and thiolate were first reported by Holm and Johnson earlier than the structural elucidation of those proteins. They synthesized a series of clusters formulated as $[Fe_4S_4(SR)_{4-n}(OCOR')_n]^{2-}$ (n = 1−4).[8] Later, Holm and Weigel[9] and Nolte et al.[10] respectively synthesized the clusters having one carboxylate and three thiolates by taking advantages of tridentate thiolate ligands, and their redox properties were analyzed. However, their structural details were not elucidated, although Holm and Weigel suggested the η^2-coordination

Received: July 9, 2013
Published: October 8, 2013

   dx.doi.org/10.1021/ic4017596 | *Inorg. Chem.* 2013, 52, 11997−12004

geometry for the acetate at the unique iron site according to the IR spectra.[9]

Recently, we designed new trithiols $Temp(SH)_3$ and $Tefp(SH)_3$ suited for the production of [3:1] site-differentiated [4Fe–4S] clusters and demonstrated their usefulness for model studies of the various site-differentiated [4Fe–4S] clusters in organisms via synthesis of these clusters having ethanethiolate, benzenethiolate, and hydrosulfide at the unique iron sites (Chart 2).[11] All of these clusters were obtained as single crystals

Chart 2

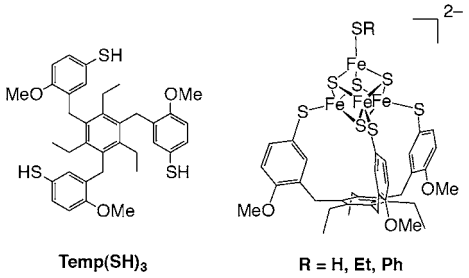

suitable for X-ray structural analysis. Herein, we report the synthesis of the model clusters having a tridentate thiolate $TempS_3^{3-}$ and a carboxylate.

RESULTS AND DISCUSSION

Synthesis of Acetate Coordinated [3:1] Site-Differentiated [4Fe–4S] Clusters. The syntheses of the carboxylate clusters were examined by the reaction of the ethanethiolate adduct $(PPh_4)_2[Fe_4S_4(SEt)(TempS_3)]$ (**1**)[11] with carboxylic acids. The addition of 4.5 equiv of acetic acid to **1** in acetonitrile and successive slow evaporation allowed the removal of volatile ethanethiol to give the acetate cluster $[PPh_4]_2[Fe_4S_4(OCOCH_3)(TempS_3)]$ (**2**) in 67% yield (Scheme 1). ESI-MS spectra confirm the formulation, and the IR spectrum shows the two CO_2^- stretching bands at 1571 and 1373 cm^{-1}.

Scheme 1. Synthesis of the Acetate Cluster 2

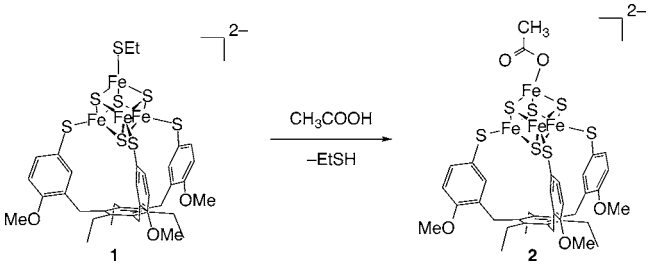

Several other carboxylate clusters were also synthesized by a similar procedure (Scheme 2). Reactions with acrylic acid, propiolic acid, maleic acid, and benzoic acid gave the corresponding carboxylate adducts **3**–**6**, respectively. To synthesize the model clusters found for aconitase[5b,f] and radical SAM enzymes,[7b,c,e,f] salicylic acid, anthranilic acid, and pyrrole-2-carboxylic acid were also reacted with **1**, which gave the corresponding carboxylate adducts **7**–**9**. The CO_2^- stretching frequencies of clusters **2**–**4** and **6**–**9** analyzed from IR spectra are summarized in the Supporting Information. The symmetric stretching bands were observed between 1313 and 1406 cm^{-1}, while the asymmetric bands were found between 1557 and

Scheme 2. Synthesis of 3–9

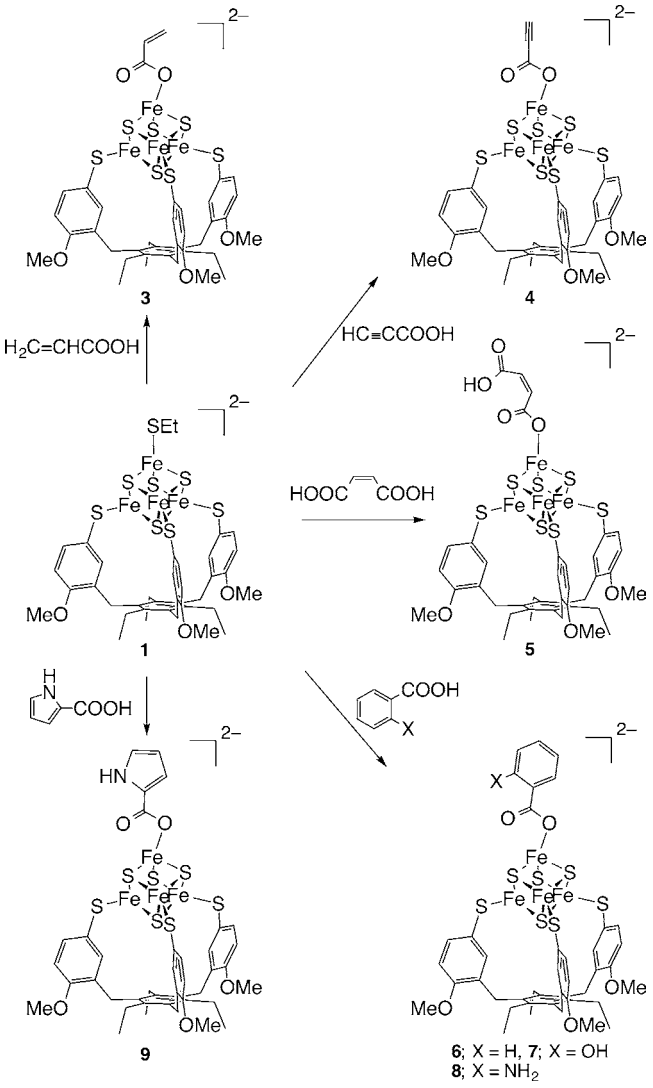

1622 cm^{-1}. The spectra for **6** and **8** were also collected in acetonitrile solution, in which the CO_2^- stretching frequencies were almost identical to those measured as KBr disks.

X-Ray Structural Analysis of 2–9. The molecular structures of **2**–**9** were analyzed using X-ray crystallography. The molecular structures and the selected metric parameters of **2**, **4**, **5**, **7**, and **9** are shown in Figure 1 and Table 1.[12]

As is evident in Figure 1, three irons of the [4Fe–4S] cores are capped by the tridentate $TempS_3^{3-}$, and the carboxylate ligands coordinate to the unique iron sites. Despite the uniqueness of the Fe1 sites due to the carboxylate coordination, the Fe–Fe and Fe–S distances around Fe1 are almost identical with those of other irons, and the metric parameters for cubane cores also resemble those of the ethanethiolate cluster **1**.[11] The coordination mode of the carboxylates is notable. As summarized in Table 1, the Fe1–O4 distances are 1.94–2.02 Å and 0.7–1.0 Å shorter than the Fe1–O5 distances with 2.65–3.12 Å. Although the Fe1–O5 distances are shorter than the sum of the van der Waals radii estimated as 3.5 Å,[13] their parameters are similar to the reported iron η^1-carboxylate complexes.[14] Thus, the carboxylate coordination to each unique iron would be regarded as η^1 via O4 rather than η^2. The O5

dx.doi.org/10.1021/ic4017596 | Inorg. Chem. 2013, 52, 11997–12004

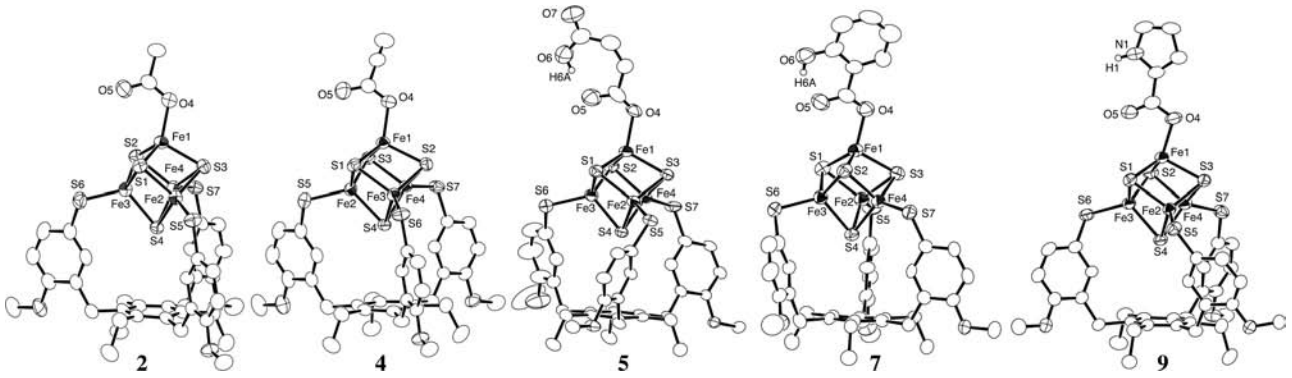

Figure 1. Molecular structures of the anion of **2**, **4**, **5**, **7**, and **9** with 50% thermal ellipsoids.

Table 1. Selected Interatomic Distances (Å) and Angles (deg) for 2, 4, 5, 7, and 9

	2	4	5	7	9
Fe1−Fe2	2.7745(13)	2.7259(7)	2.7427(18)	2.7632(15)	2.7663(10)
Fe1−Fe3	2.7395(13)	2.7603(7)	2.7301(18)	2.7447(15)	2.7362(11)
Fe1−Fe4	2.7356(13)	2.7277(8)	2.7514(17)	2.7708(14)	2.7550(9)
Fe2−Fe3	2.7384(13)	2.7406(7)	2.756(2)	2.7864(15)	2.7740(10)
Fe2−Fe4	2.7549(12)	2.7385(7)	2.7345(18)	2.7375(14)	2.7170(10)
Fe3−Fe4	2.7383(13)	2.7616(7)	2.7310(16)	2.7591(14)	2.7300(10)
Fe1−S1	2.2359(19)	2.2308(10)	2.258(3)	2.253(2)	2.2739(17)
Fe1−S2	2.2987(18)	2.3030(10)	2.294(3)	2.278(2)	2.2953(16)
Fe1−S3	2.3138(18)	2.3060(10)	2.310(2)	2.297(2)	2.3400(12)
Fe2−S1	2.3148(18)	2.3211(10)	2.301(2)	2.306(2)	2.3095(12)
Fe2−S3	2.2453(19)	2.2310(10)	2.260(2)	2.243(2)	2.2624(16)
Fe2−S4	2.3075(17)	2.3034(10)	2.293(3)	2.2819(19)	2.2881(15)
Fe3−S1	2.3191(17)	2.3146(10)	2.301(3)	2.287(2)	2.3033(15)
Fe3−S2	2.2300(18)	2.2557(10)	2.267(3)	2.268(2)	2.2619(16)
Fe3−S4	2.3031(17)	2.3108(10)	2.294(2)	2.3120(19)	2.3010(12)
Fe4−S2	2.2960(18)	2.3132(10)	2.301(2)	2.306(2)	2.3085(13)
Fe4−S3	2.3095(17)	2.2985(10)	2.306(3)	2.280(2)	2.2864(16)
Fe4−S4	2.2399(18)	2.2405(10)	2.252(2)	2.2574(19)	2.2484(17)
Fe2−S5	2.269(2)	2.2487(12)	2.255(3)	2.269(2)	2.2713(15)
Fe3−S6	2.260(3)	2.2650(12)	2.257(3)	2.276(2)	2.2601(19)
Fe4−S7	2.2765(18)	2.2788(10)	2.261(2)	2.266(2)	2.2616(15)
Fe1−O4	1.944(5)	1.958(3)	2.020(7)	1.997(5)	1.974(5)
Fe1−O5	2.996(6)	3.120(4)	3.089(8)	2.883(6)	2.652(4)
O4−C85	1.279(9)	1.280(5)	1.140(14)	1.181(10)	1.288(6)
O5−C85	1.230(9)	1.223(5)	1.265(14)	1.252(11)	1.221(9)
O5−O6			2.497(12)	2.552(9)	

atoms of the carboxylates are commonly pointing to the middle of the two S atoms of the cubane cores to avoid steric repulsion.

The difference between the two C−O bond distances of the carboxylate ligands is also notable. While the C85−O4 bonds regarded as single bonds are reasonably longer than the double-bond-like C85−O5 bonds for **2**, **4**, and **9**, the C85−O4 bonds of **5** and **7** are shorter than the C85−O5 bonds, probably due to the hydrogen bonding interaction between the terminal carboxylic acid for **5** and the hydroxyl group for **7**. As for **9**, intermolecular hydrogen bonding was formed as shown in Figure 2, as indicated by the intermolecular N···O distance of 2.845 Å.[15] However, due to the low acidity of the pyrrole, long−short alternation for the carboxylate C−O bonds was not observed.

Structural Comparison of the Model Clusters and Those in Metalloproteins. As is evident in the structures in Figure 1, the carboxylates used herein commonly coordinate to the iron at their carboxylate moieties exclusively in an η^1 manner. This coordination mode conforms to those observed for the [4Fe−4S] clusters in DPOR, *Pf* ferredoxin, and IspG (Chart 1).[3c,4d,6a] On the other hand, it is dissimilar to the chelate binding observed for aconitase or radical SAM superfamily enzymes (Chart 1),[5b,f,7b,c,e,f] although the carboxylates of **3**, **4**, **7**, **8**, and **9** have additional auxiliaries potentially able to coordinate to the iron, such as alkene, alkyne, hydroxy group, amino group, and pyrrole. The reasons for the different

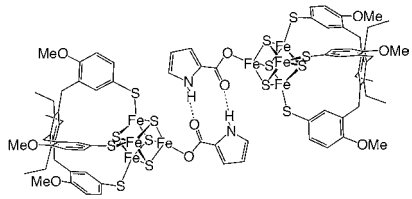

Figure 2. Intermolecular hydrogen bonding interaction of **9**.

dx.doi.org/10.1021/ic4017596 | *Inorg. Chem.* 2013, 52, 11997−12004

coordination are not clear, but a possible explanation is that the oxidation state of the [4Fe−4S] clusters in aconitase, and radical SAM superfamily enzymes might be in the oxidized $[4Fe-4S]^{3+}$ state. Previously, we reported the structure of the site-differentiated $[4Fe-4S]^{3+}$ cluster $[Fe_4S_4(SDmp)_3(thf)_3]$,[16] in which the unique iron site is coordinated by three THF oxygen atoms to assume an octahedral geometry, while the other three irons have monodentate bulky thiolates $DmpS^-$ (Dmp = 2,6-dimesitylphenyl). Another explanation is that the hydroxyl of citrate/isocitrate of aconitase and amine of SAM of radical SAM superfamily enzymes might be more anionic through the hydrogen bonding network with the surrounding protein. Further model synthesis and structural elucidation is needed to elucidate the nature of the clusters in the enzymes.

Redox Properties of 2−9. The cyclic voltammograms (CVs) of **2**−**9** recorded in a 0.1 M n-Bu_4NPF_6 acetonitrile solution have revealed the redox properties. As shown in Figure 3, cluster **2** displays one reversible $[Fe_4S_4]^{2+}/[Fe_4S_4]^{+}$ redox at

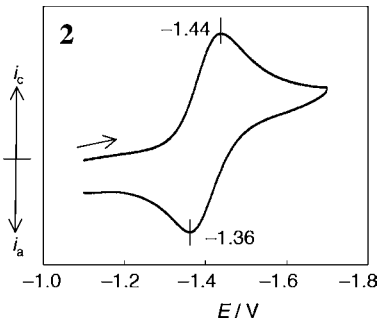

Figure 3. Cyclic voltammogram of **2**.

$E_{1/2}$ = −1.40 V vs Ag/Ag^+. Clusters **3**, **6**, and **9** also show similar redox waves at −1.43, −1.40, and −1.41 V, respectively (Table 2).[17] These potentials are significantly positive compared to that of the ethanethiolate cluster **1** observed at −1.49 V,[11] and this positive shift is common with the similar [4Fe−4S] clusters having a tridentate thiolate and an acetate previously reported by Holm et al.[9,18] and Nolte et al.[10,19]

However, the CV spectra of **4**, **5**, **7**, and **8** coordinated respectively by propiolate, maleate, salicylate, and anthranilate are rather complicated, as shown in Figure 4. Cluster **8** appears to show the redox process at $E_{1/2}$ = −1.40 V, but the i_a for this reverse oxidation process appears smaller. In addition to this fact, a smaller reversible redox couple was observed at $E_{1/2}$ = −1.13 V. Similarly, **5** and **7** also show two redox processes, although the reversibility and relative intensity of the two reduction waves vary. When the CV of **8** was recorded in the presence of excess $(NEt_4)(OCOC_6H_4NH_2)$, the reversibility of the negative redox process was significantly improved, and concomitantly the smaller redox couple at $E_{1/2}$ = −1.13 V had disappeared. The same spectral change was also observed for **7**. This result indicates that for **8** the redox at $E_{1/2}$ = −1.40 V is assignable the carboxylate cluster **8** and that the carboxylate ligand dissociates from the cluster upon reduction. In the cases of **5** and **7**, a similar carboxylate-dissociation would have occurred, which could result in the complex CV spectra. For the cases of **5**, **7**, and **8**, the facile dissociation of the carboxylate ligands would be partly attributable to the intramolecular hydrogen bondings that stabilize the dissociated carboxylates, although the reason for the irreversibility of **4** has not been clear. The species that gave a redox process at around $E_{1/2}$ = −1.13 V was not characterized, but this potential suggests the formation of a cluster having a charge-neutral ligand in addition to the tridentate thiolate.[20] A plausible structure could be the acetonitrile adduct.

When we collected the CV data for **6** and **8** in THF, the reversibility for the $[Fe_4S_4]^{2+}/[Fe_4S_4]^{+}$ redox was considerably improved and became reversible in CH_2Cl_2. The results suggest that the dissociation of the carboxylate ligands is promoted in the polar and highly coordinating solvent.

Previously, Nakamura et al. reported the effect of the hydrogen bonding interation toward the thiolate ligand S for the [4Fe−4S] clusters having four thiolate ligands.[21] In their case, the significant negative shift for the $[Fe_4S_4]^{2+}/[Fe_4S_4]^{+}$ redox potential was observed via the hydrogen bonding interaction because the donation from the thiolate ligands became weaker. Similarly, the coordination of the carboxylate became weaker in our case, although the redox potentials of **7** and **8** are similar to the value of **6**.

Redox Properties of the Model Clusters and the Clusters in Metalloproteins. The redox potentials of the carboxylate clusters **2**−**9** exhibit a significant positive shift from that of the thiolate cluster **1**, and thus the carboxylate clusters function as better electron acceptors. This redox property conforms to the arrangement of the [4Fe−4S] clusters in the electron transfer systems included in DPOR,[4] where the electron flows from the all-cysteine [4Fe−4S] cluster to the active site through the aspartate [4Fe−4S] cluster shown in Chart 1.[22] A similar electron relay is also included in formaldehyde oxidoreductase (FOR) with *Pf* ferredoxin,[3] in which electrons flow in an opposite direction from the active site to cysteine cluster, and farther to the aspartate cluster.[23]

It is also notable that the reduction potential of WT *Pf* ferredoxin at E_m = −368 mV showed a 58 mV negative shift upon mutation of aspartate to cysteine coordinated to the unique iron site of the cluster.[3b] The shift of the potential is similar to the values for our model clusters (ΔE = 60−120 mV). It was also reported that no activity was found for the D36C DPOR mutant,[4d] which contains an all-cysteine cluster instead of the aspartate cluster (Chart 1). A conceivable reason is that the electron transfer is blocked between the two [4Fe−4S] clusters according to our results.

Table 2. Redox Potentials of 2−9[a]

	E_{pc}/V	E_{pa}/V	$E_{1/2}$/V
2	−1.44	−1.36	−1.40
3	−1.47	−1.39	−1.43
4	−1.40		
5	−1.44	−1.34	−1.39
	−1.15	−1.08	−1.12
6	−1.43	−1.36	−1.40
7	−1.41		
	−1.20	−1.09	−1.15
7 with 20 mM $(NEt_4)(OCOC_6H_4OH)$	−1.41	−1.32	−1.37
		−1.09	
8	−1.45	−1.35	−1.40
	−1.16	−1.09	−1.13
8 with 20 mM $(NEt_4)(OCOC_6H_4NH_2)$	−1.45	−1.34	−1.40
9	−1.45	−1.36	−1.41

[a]The data were recorded in a 0.1 M n-Bu_4NPF_6 solution (CH_3CN) with a glassy carbon working electrode, a Pt counter electrode, and a $Ag/AgNO_3$ reference electrode. The scan rate was 0.1 V s^{-1}.

dx.doi.org/10.1021/ic4017596 | *Inorg. Chem.* 2013, 52, 11997−12004

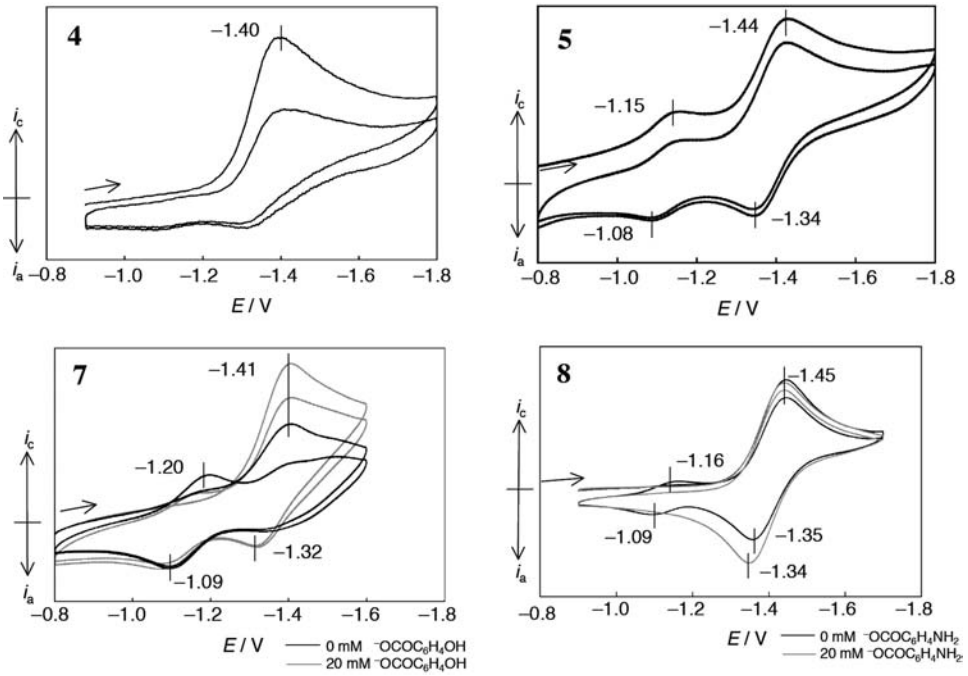

Figure 4. Cyclic voltammogram of **4**, **5**, **7**, and **8**.

CONCLUSION

We synthesized a series of [4Fe−4S] clusters coordinated by three thiolates and one carboxylate. The model studies provided us with various important pieces of information. An important achievement is that the carboxylate coordination geometry was confirmed by X-ray structural analysis, in which the carboxylates would be commonly coordinated to the unique iron site in η^1 rather than an η^2 manner, and it conforms to similar protein structures. Because the CO_2^- stretching frequencies from a KBr disk and acetonitrile solution are almost identical, the coordination mode would be retained even in the solution. Another achievement resides in the redox potentials for the $[4Fe-4S]^{2+/1+}$ process. The positively shifted potential of the carboxylate clusters conforms to the arrangement of the thiolate and carboxylate clusters in the electron relay systems.

EXPERIMENTAL SECTION

General Procedures. All compounds were handled under an atmosphere of pure nitrogen using standard Schlenk techniques or glove boxes. Hexane, ether, THF, acetonitrile, dichloromethane, and DMF were degassed and purified by the method described by Grubbs, in which the solvents were passed over columns of activated alumina and a copper catalyst supplied by Hansen & Co. Ltd. ^{1}H NMR spectra were acquired by using a JEOL ECA-600. NMR assignments were supported by the additional 2D NMR experiments. Cyclic voltammograms were recorded on a BAS-ALS-660A electron analyzer using a glassy carbon working electrode and 0.1 M (CH_3CN, CH_2Cl_2) or 0.2 M (THF) n-Bu_4NPF_6 as the supporting electrolyte, in which the potentials are referred to the $Ag/AgNO_3$ electrode. Electrospray ionization time-of-flight mass spectrometry (ESI-TOF-MS) spectra were obtained from a Micromass LCT TOF-MS spectrometer or Bruker microTOF II-NUT. Infrared spectra were recorded with a JASCO FT/IR-410. UV/vis spectra were recorded in 10-mm quartz glass cells with a JASCO V560 spectrometer. Elemental analyses were performed on a LECO−CHNS-932 elemental analyzer or Elementar Analysensysteme GmbH varioMICRO, where the samples were sealed in tin or silver capsules under nitrogen. $(PPh_4)_2[Fe_4S_4(SEt)(TempS_3)]$ (**1**) was synthesized according to the previous reports.[11]

Synthesis of $(PPh_4)_2[Fe_4S_4(OCOCH_3)(TempS_3)]$ (2). Acetic acid in acetonitrile (0.17 M, 2.3 mL, 0.40 mmol) was added to **1** (150 mg, 0.088 mmol) in acetonitrile (30 mL) and stirred for 4 h. After removal of all the volatiles in vacuo very slowly, the residue was washed by ether and THF mixture solvent and extracted by acetonitrile (15 mL). Removal of the solvent in vacuo gave **2** as a black powder (100 mg, 0.059 mmol, 67% yield). Layering hexane and ether onto an acetonitrile solution of **2** gave black plate crystals. Anal. Calcd for $C_{86}Fe_4S_7H_{82}O_5P_2{\cdot}C_2H_3N{\cdot}C_{1.5}H_{3.5}$: C, 60.80; H, 5.05; N, 0.79; S, 12.70. Found: C, 61.15; H, 5.25; N, 0.84; S, 12.31. ^{1}H NMR (CD_3CN, δ): 7.89 (s, $P(C_6H_5)_4$), 7.72−7.58 (m, arom + $P(C_6H_5)_4$), 6.30 (br, arom), 5.55 (br, arom), 4.58 (s, $OCOCH_3$), 3.99 (s, OCH_3), 3.37 (s, CH_2), 2.32 (br, CH_2CH_3), 1.11 (t, CH_2CH_3, 9H). Cyclic voltammetry (CH_3CN, 0.1 V/s): $E_{1/2}$ = −1.40 V, (THF, 0.1 V/s); $E_{1/2}$ = −1.54. UV/vis (CH_3CN): λ_{max} [nm] (ε [$cm^{-1}{\cdot}M^{-1}$]) = 456 (1.2×10^4), 299 (2.0×10^4) sh. IR (KBr): $\nu(COO^-)$ = 1571, 1373 cm^{-1}.

Synthesis of $(PPh_4)_2[Fe_4S_4(OCOCH{=}CH_2)(TempS_3)]$ (3). Cluster **3** was synthesized as described for **2** from **1** (91 mg, 0.053 mmol) and acrylic acid (0.26 M, 0.22 mL, 0.057 mmol) in 38% yield as black microcrystals (35 mg, 0.020 mmol). Anal. Calcd for $C_{87}Fe_4S_7H_{82}O_5P_2$: C, 60.85; H, 4.81; S, 13.07. Found: C, 60.95; H, 4.85; S, 12.97. ^{1}H NMR (CD_3CN, δ): 8.23 (br, $OCOCH{=}CH_2$), 7.90 (s, $P(C_6H_5)_4$), 7.72−7.65 (m, arom + $P(C_6H_5)_4$), 6.32 (br, arom), 6.02 (br, $OCOCH{=}CH_2$), 5.66 (br, $OCOCH{=}CH_2$), 5.55 (br, arom), 3.99 (s, OCH_3), 3.37 (s, CH_2), 2.32 (br, CH_2CH_3), 1.12 (t, CH_2CH_3). Cyclic voltammetry (CH_3CN, 0.1 V/s): $E_{1/2}$ = −1.43 V. UV/vis (CH_3CN): λ_{max} [nm] (ε [$cm^{-1}{\cdot}M^{-1}$]) = 466 (9.4×10^3), 361 (1.1×10^4) sh., 294 (1.9×10^4) sh. IR (KBr); $\nu(COO^-)$ = 1557, 1406 cm^{-1}.

Synthesis of $(PPh_4)_2[Fe_4S_4(OCOC{\equiv}CH)(TempS_3)]$ (4). Cluster **4** was synthesized as described for **2** from **1** (160 mg, 0.093 mmol) and propiolic acid (0.16 M, 1.2 mL, 0.19 mmol) in 80% yield as crystals (128 mg, 0.075 mmol). Anal. Calcd for $C_{87}Fe_4S_7H_{80}O_5P_2{\cdot}C_2H_3N{\cdot}C_{1.5}H_{3.5}$: C, 61.14; H, 4.90; N, 0.79; S, 12.62. Found: C, 61.53; H, 5.16; N, 0.81; S, 11.72. Cyclic voltammetry (CH_3CN, 0.1 V/s): E_{pc} = −1.40 V. IR (KBr): $\nu(COO^-)$ = 1615, 1313 cm^{-1}, $\nu(C{\equiv}C)$ = 2091 cm^{-1}.

Synthesis of $(PPh_4)_2[Fe_4S_4(OCOCH{=}CH(cis\text{-}COOH))(TempS_3)]$ (5). Cluster **5** was synthesized as described for **2** from **1** (150 mg, 0.088 mmol) and maleic acid (0.018 M, 5.0 mL, 0.090 mmol) in 15% yield as crystals (24 mg, 0.014 mmol), except for using acetonitrile and DMF solution of **5** in crystallization. Anal. Calcd for

dx.doi.org/10.1021/ic4017596 | Inorg. Chem. 2013, 52, 11997−12004

Table 3. Crystal Data of 2, 4, 5, 7, and 9

	2·(CH_3CN·0.25C_6H_{14})	**4**·(CH_3CN·0.25C_6H_{14})	**5**·2(DMF)	**7**	**9**·(CH_3CN)
formula	$C_{86}Fe_4S_7H_{82}O_5P_2$·$C_2H_3N$·$C_{1.5}H_{3.5}$	$C_{87}Fe_4S_7H_{80}O_5P_2$·$C_2H_3N$·$C_{1.5}H_{3.5}$	$C_{88}Fe_4S_7H_{82}O_7P_2$·$C_6H_{14}O_2N_2$	$C_{91}Fe_4S_7H_{84}O_6P_2$	$C_{89}Fe_4S_7H_{83}O_5NP_2$·$C_2H_3N$
weight	1767.94	1777.94	1907.56	1783.42	1797.45
cryst syst	monoclinic	monoclinic	monoclinic	monoclinic	monoclinic
space group	$P2_1/c$ (#14)	$P2_1/c$ (#14)	$P2_1/n$ (#14)	$P2_1/n$ (#14)	$P2_1/c$ (#14)
a/Å	21.157(3)	21.208(3)	21.004(5)	13.033(2)	30.000(4)
b/Å	14.060(2)	14.108(2)	12.963(3)	25.109(4)	13.037(2)
c/Å	28.020(4)	28.139(4)	34.035(8)	25.071(4)	23.319(3)
β/deg	91.294(2)	90.578(3)	105.483(4)	91.042(4)	111.7250(10)
V/Å^3	8333(2)	8419(2)	8931(4)	8203(2)	8473(2)
Z	4	4	4	4	4
D_{calc}/g cm^{-1}	1.409	1.403	1.419	1.444	1.409
μ/cm^{-1}	9.482	9.390	8.940	9.646	9.343
$F(000)$	3674.00	3690.00	3968.00	3696.00	3728.00
$2\theta_{max}$/deg	55.0	55.0	50.0	55.0	55.0
no. reflns collected	58477	101389	58300	66980	67501
independent reflns	18769	19266	15753	18411	19364
number of params	980	1007	1045	998	997
$R1$ $[I > 2\sigma(I)]^a$	0.0781	0.0553	0.1105	0.0866	0.0721
$wR2$ $[I > 2\sigma(I)]^b$	0.02678	0.1647	0.3278	0.2866	0.241
GOF^c	1.067	1.186	1.049	1.049	1.059
CCDC	949114	949115	949116	949117	949118

$^a R1 = ||F_o| - |F_c||/\Sigma|F_o|$ $(I > 2\sigma(I))$. $^b wR2 = \{[\Sigma w(|F_o| - |F_c|)^2/\Sigma wF_o^2]\}^{1/2}$ (all data). $^c GOF = [\Sigma w(|F_o| - |F_c|)^2/(N_o - N_v)]^{1/2}$ (N_o = number of observations, N_v = number of variables).

$C_{88}Fe_4S_7H_{82}O_7P_2$: C, 60.01; H, 4.69; S, 12.74. Found: C, 60.08; H, 5.18; S, 12.89. ^{1}H NMR (CD_3CN, δ): 7.90 (s, P(C_6H_5)$_4$), 7.72−7.65 (m, arom + P(C_6H_5)$_4$), 6.34 (br, arom), 5.60 (br, arom), 3.99 (s, OCH_3), 3.37 (s, CH_2), 2.32 (br, CH_2CH_3), 1.13 (s, CH_2CH_3). The protons of carboxylate ligand were not assignable. Cyclic voltammetry (CH_3CN, 0.1 V/s): $E_{1/2}$ = −1.12, −1.39 V. UV/vis (CH_3CN): λ_{max} [nm] (ε [cm^{-1}·M^{-1}]) = 472 (1.4 × 10^4), 363 (1.7 × 10^4) sh, 288 (2.5 × 10^4).

Synthesis of (PPh$_4$)$_2$[Fe$_4$S$_4$(OCOC$_6$H$_5$)(TempS$_3$)] (6). Cluster **6** was synthesized as described for **2** from **1** (95 mg, 0.056 mmol) and benzoic acid (0.046 M, 1.5 mL, 0.069 mmol) in 38% yield as black microcrystals (38 mg, 0.022 mmol). Anal. Calcd for $C_{91}Fe_4S_7H_{84}O_5P_2$: C, 61.84; H, 4.79; S, 12.70. Found: C, 61.60; H, 4.90; S, 12.60. ^{1}H NMR (CD_3CN, δ): 8.13 (br, OCOC$_6H_5$), 7.90 (t, P(C_6H_5)$_4$), 7.72−7.64 (m, arom + P(C_6H_5)$_4$), 7.57 (br, OCOC$_6H_5$), 7.27 (br, OCOC$_6H_5$), 6.33 (br, arom), 5.59 (br, arom), 4.00 (s, OCH_3), 3.38 (s, CH_2), 2.32 (br, CH_2CH_3), 1.13 (s, CH_2CH_3). Cyclic voltammetry (CH_3CN, 0.1 V/s): $E_{1/2}$ = −1.40 V, (THF, 0.5 V/s); $E_{1/2}$ = −0.31, −1.53 V attributable to the $[Fe_4S_4]^{2+}/[Fe_4S_4]^{3+}$ and $[Fe_4S_4]^{2+}/[Fe_4S_4]^{+}$ processes, (CH_2Cl_2, 0.1 V/s); $E_{1/2}$ = −0.24, −1.48 V attributable to the $[Fe_4S_4]^{2+}/[Fe_4S_4]^{3+}$ and $[Fe_4S_4]^{2+}/[Fe_4S_4]^{+}$ processes. UV/vis (CH_3CN): λ_{max} [nm] (ε [cm^{-1}·M^{-1}]) = 462 (1.1 × 10^4), 354 (1.4 × 10^4) sh, 297 (2.1 × 10^4) sh. IR (KBr): ν(COO$^-$) = 1622, 1322 cm^{-1}.

Synthesis of [PPh$_4$]$_2$[Fe$_4$S$_4$(OCOC$_6$H$_4$(*o*-OH))(TempS$_3$)] (7). Cluster **7** was synthesized as described for **2** from **1** (100 mg, 0.059 mmol) and salicylic acid (0.012 M, 5.0 mL, 0.059 mmol) in 65% yield as black crystals (68 mg, 0.038 mmol). Anal. Calcd for $C_{91}Fe_4S_7H_{84}O_6P_2$: C, 61.29; H, 4.75; S, 12.59. Found: C, 61.01; H, 4.84; S, 12.42. ^{1}H NMR (CD_3CN, δ): 8.07 (br, OCOC$_6H_4$OH), 7.88 (t, P(C_6H_5)$_4$), 7.80−7.63 (m, arom + P(C_6H_5)$_4$), 7.13 (br, OCOC$_6H_4$OH), 6.93 (br, OCOC$_6H_4$OH), 6.35 (br, arom), 5.58 (br, arom), 4.00 (s, OCH_3), 3.41 (s, CH_2), 2.33 (br, CH_2CH_3), 1.13 (s, CH_2CH_3). Some protons of carboxylate ligand were not assignable. Cyclic voltammetry (CH_3CN, 0.1 V/s): $E_{1/2}$ = −1.15 V, E_{pc} = −1.41 V, (the presence of 20 mM (NEt_4)(OCOC$_6H_4$OH) in CH_3CN, 0.1 V/s); $E_{1/2}$ = −1.37 V, E_{pa} = −1.09 V. UV/vis (CH_3CN): λ_{max} [nm] (ε [cm^{-1}·M^{-1}]) = 461 (1.1 × 10^4), 296 (2.3 × 10^4). IR (KBr): ν(COO$^-$) = 1597, 1361 cm^{-1}.

Synthesis of (PPh$_4$)$_2$[Fe$_4$S$_4$(OCOC$_6$H$_4$(*o*-NH$_2$))(TempS$_3$)] (8). Cluster **8** was synthesized as described for **2** from **1** (100 mg, 0.059 mmol) and anthranilic acid (0.055 M, 1.3 mL, 0.072 mmol) in 47% yield as black crystalline powder (49 mg, 0.028 mmol). Anal. Calcd for $C_{91}Fe_4S_7H_{85}O_5NP_2$: C, 61.32; H, 4.81; N, 0.79; S, 12.59. Found: C, 61.04; H, 5.00; N, 1.17; S, 12.38. ^{1}H NMR (CD_3CN, δ): 8.10 (br, OCOC$_6H_4$NH$_2$), 7.90 (t, P(C_6H_5)$_4$), 7.72−7.64 (m, arom + P(C_6H_5)$_4$), 6.94 (br, OCOC$_6H_4$NH$_2$), 6.72 (br, OCOC$_6H_4$NH$_2$), 6.33 (br, arom), 6.13 (br, OCOC$_6H_4$NH$_2$), 5.58 (br, arom), 4.00 (s, OCH_3), 3.37 (s, CH_2), 2.32 (br, CH_2CH_3), 1.11 (t, CH_2CH_3). Some protons of the carboxylate ligand were not assignable. Cyclic voltammetry (CH_3CN, 0.1 V/s): $E_{1/2}$ = −1.13, −1.40 V, (the presence of 20 mM (NEt_4)(OCOC$_6H_4$NH$_2$) in CH_3CN, 0.1 V/s); $E_{1/2}$ = −1.40 V, (THF, 0.5 V/s); $E_{1/2}$ = −0.38, −1.57 V attributable to the $[Fe_4S_4]^{2+}/[Fe_4S_4]^{3+}$ and $[Fe_4S_4]^{2+}/[Fe_4S_4]^{+}$ processes, (CH_2Cl_2, 0.1 V/s); $E_{1/2}$ = −0.26, −1.48 V attributable to the $[Fe_4S_4]^{2+}/[Fe_4S_4]^{3+}$ and $[Fe_4S_4]^{2+}/[Fe_4S_4]^{+}$ processes. UV/vis (CH_3CN): λ_{max} [nm] (ε [cm^{-1}·M^{-1}]) = 458 (1.6 × 10^4), 295 (3.1 × 10^4). IR (KBr): ν(COO$^-$) = 1612, 1340 cm^{-1}.

Synthesis of (PPh$_4$)$_2$[Fe$_4$S$_4$(OCO(NC$_4$H$_4$))(TempS$_3$)] (9). Cluster **9** was synthesized as described for **2** from **1** (82 mg, 0.048 mmol) and pyrrole-2-carboxylic acid (0.035 M, 1.65 mL, 0.058 mmol) in 33% yield as black crystalline powder (28 mg, 0.016 mmol). Anal. Calcd for $C_{89}Fe_4S_7H_{83}O_5NP_2$: C, 60.86; H, 4.76; N, 0.80; S, 12.78. Found: C, 60.37; H, 4.65; N, 0.99; S, 12.32. ^{1}H NMR (CD_3CN, δ): 7.88 (s, P(C_6H_5)$_4$), 7.70−7.63 (m, arom + P(C_6H_5)$_4$), 6.54 (br, OCOC$_4H_3$NH), 6.46 (br, OCOC$_4H_3$NH), 6.32 (br, arom), 6.28 (br, OCOC$_4H_3$NH), 5.55 (br, arom), 3.99 (s, OCH_3), 3.37 (s, CH_2), 2.32 (br, CH_2CH_3), 1.11 (s, CH_2CH_3). One proton of the carboxylate ligand was not assignable. Cyclic voltammetry (CH_3CN, 0.1 V/s): $E_{1/2}$ = −1.41 V. UV/vis (CH_3CN): λ_{max} [nm] (ε [cm^{-1}·M^{-1}]) = 457 (1.5 × 10^4), 361 (2.0 × 10^4) sh, 295 (3.5 × 10^4) sh. IR (KBr): ν(COO$^-$) = 1559, 1352 cm^{-1}.

Crystal-Structure Determination. Crystal data and refinement parameters for the clusters reported herein are summarized in Table 3. Single crystals were mounted on a loop using oil (Paraton, Hampton

dx.doi.org/10.1021/ic4017596 | Inorg. Chem. 2013, 52, 11997−12004

Research Corp.). Diffraction data were collected at −100 °C under a cold nitrogen stream on a Rigaku Micromax-007 instrument with a Saturn 70 CCD area detector (for **4**), or on a Rigaku FR-E instrument with a Saturn 70 CCD detector (for **2**, **5**, **7**, and **9**) using graphite-monochromated Mo Ka radiation (λ = 0.710690 Å). Using an oscillation range of 0.5°, 1080 data images were collected for **4**, while 720 images were measured for **2**, **5**, **7**, and **9**. The data were integrated and corrected for absorption using the Rigaku/MSC CrystalClear program package. The structures were solved using a direct method (SIR92 for **4**, **5**; SIR97 for **7**; SHELXS97 for **2**, **9**) and were refined by full-matrix least-squares on F^2 by the Rigaku/MSC CrystalStructure program package. Anisotropic refinement was applied to all non-hydrogen atoms except for disordered atoms and several crystal solvents. All the hydrogen atoms were put at the calculated positions, especially using the HFIX147 method for the H6A atom of **5** and H6 atom of **7**. In **5**, a phenyl group of PPh_4^+ is disordered over two positions in a 1:1 ratio, and an anisole group of tridentate thiolate is disordered. Acetonitrile molecules of **2** and **9** are disordered over two positions in a 2:1 and 1:1 ratio, respectively.

■ ASSOCIATED CONTENT

Ⓢ Supporting Information

Crystallographic data in CIF format for **2**, **4**, **5**, **7**, and **9**; table of the CO_2^- stretching frequencies of for **2**−**5** and **6**−**9**; molecular structures of **3**, **6**, and **8**; CV data for **3**, **6**, and **9**. This material is available free of charge via the Internet at http://pubs.acs.org.

■ AUTHOR INFORMATION

Corresponding Authors

*(T.M.) E-mail: tmatsu@chem.nagoya-u.ac.jp. Fax: Int. code: +81-52-789-2943.

* (K.T.) E-mail: i45100a@nucc.cc.nagoya-u.ac.jp. Fax: Int. code: +81-52-789-2943.

Notes

The authors declare no competing financial interest.

■ ACKNOWLEDGMENTS

This research was financially supported by Grant-in-Aids for Scientific Research (Nos. 23000007 and 25410066) from the Ministry of Education, Culture, Sports, Science, and Technology, Japan.

■ DEDICATION

Dedicated to Prof. Dr. Renji Okazaki on the occasion of his 77th birthday.

■ REFERENCES

(1) (a) Bertini, I.; Sigel, A.; Sigel, H. *Handbook on Metalloproteins*; Marcel Dekker: New York, 2001; Chapter 10. (b) Messerchmidt, A.; Huber, R.; Poulos, T.; Wiehardt, K. *Handbook of Metalloproteins Vol. 1*; John Wiley & Sons: Chichester, U. K., 2001; pp 543−552, 560−609.

(2) (a) Messerchmidt, A.; Huber, R.; Poulos, T.; Wiehardt, K. *Handbook of Metalloproteins Vol. 1*; John Wiley & Sons: Chichester, U. K., 2001; pp 471−485. (b) Messerchmidt, A.; Huber, R.; Poulos, T.; Wiehardt, K. *Handbook of Metalloproteins Vol. 2*; John Wiley & Sons: Chichester, U. K., 2001; pp 738−751, 880−896. (c) Bertero, M. G.; Rothery, R. A.; Palak, M.; Hou, C.; Lim, D.; Blasco, F.; Weiner, J. H.; Strynadka, N. C. J. *Nat. Struct. Biol.* **2003**, *10*, 681−687. (d) Sazanov, L. A.; Hinchliffe, P. *Science* **2006**, *311*, 1430−1436. (e) Gräwert, T.; Span, I.; Eisenreich, W.; Rohdich, F.; Eppinger, J.; Bacher, A.; Groll, M. *Proc. Natl. Acad. Sci. U. S. A.* **2010**, *107*, 1077−1081. (f) Messerchmidt, A. *Handbook of Metalloproteins Vol. 4*; John Wiley & Sons: Chichester, U. K., 2011; pp 172−182, 397−412. (g) Knauer, S. H.; Buckel, W.; Dobbek, H. *J. Am. Chem. Soc.* **2011**, *133*, 4342−4347.

(3) (a) Zhou, Z. H.; Adams, M. W. W. *Biochemistry* **1997**, *36*, 10892−10900. (b) Brereton, P. S.; Verhagen, M. F. J. M.; Zhou, Z. H.; Adams, M. W. W. *Biochemistry* **1998**, *37*, 7351−7362. (c) Hu, Y.; Faham, S.; Roy, R.; Adams, M. W. W.; Rees, D. C. *J. Mol. Biol.* **1999**, *286*, 899−914. (d) Messerchmidt, A.; Huber, R.; Poulos, T.; Wiehardt, K. *Handbook of Metalloproteins Vol. 2*; John Wiley & Sons: Chichester, U.K., 2001; pp1086−1096.

(4) (a) Fujita, Y.; Bauer, C. E. *J. Biol. Chem.* **2000**, *275*, 23583−23588. (b) Sarma, R.; Barney, B. M.; Hamilton, T. L.; Jones, A.; Seefeldt, L. C.; Peters, J. W. *Biochemistry* **2008**, *47*, 13004−13015. (c) Nomata, J.; Ogawa, T.; Kitashima, M.; Inoue, K.; Fujita, Y. *FEBS Lett.* **2008**, *582*, 1346−1350. (d) Muraki, N.; Nomata, J.; Ebata, K.; Mizoguchi, T.; Shiba, T.; Tamiaki, H.; Kurisu, G.; Fujita, Y. *Nature* **2010**, *465*, 110−115.

(5) (a) Robbins, A. H.; Stout, C. D. *Proc. Natl. Acad. Sci. U. S. A.* **1989**, *86*, 3639−3643. (b) Lauble, H.; Kennedy, M. C.; Beinert, H.; Stout, C. D. *Biochemistry* **1992**, *31*, 2135−2748. (c) Lauble, H.; Kennedy, M. C.; Beinert, H.; Stout, C. D. *J. Mol. Biol.* **1994**, *237*, 437−451. (d) Lauble, H.; Stout, C. D. *Proteins: Struct., Funct., Genet.* **1995**, *22*, 1−11. (e) Beinert, H.; Kennedy, M. C.; Stout, C. D. *Chem. Rev.* **1996**, *96*, 2335−2373. (f) Lloyd, S. J.; Lauble, H.; Prasad, G. S.; Stout, C. D. *Protein Sci.* **1999**, *8*, 2655−2662.

(6) (a) Lee, M.; Gräwert, T.; Quitterer, F.; Rohdich, F.; Eppinger, J.; Eisenreich, W.; Bacher, A.; Groll, M. *J. Mol. Biol.* **2010**, *404*, 600−610. (b) Wang, W.; Li, J.; Wang, K.; Huang, C.; Zhang, Y.; Oldfield, E. *Proc. Natl. Acad. Sci.* **2010**, *107*, 11189−11193. (c) Xiao, Y.; Nyland, R. L., II; Meyers, C. L. F.; Liu, P. *Chem. Commun.* **2010**, *46*, 7220−7222. (d) Xu, W.; Lees, N. S.; Adedeji, D.; Wiesner, J.; Jomaa, H.; Hoffman, B. M.; Duin, E. C. *J. Am. Chem. Soc.* **2010**, *132*, 14509−14520.

(7) (a) Sofia, H. J.; Chen, G.; Hetzler, B. G.; Reyes-Spindola, J. F.; Miller, N. E. *Nucleic Acids Res.* **2001**, *29*, 1097−1106. (b) Berkovitch, F.; Nicolet, Y.; Wan, J. T.; Jarrett, J. T.; Drennan, C. L. *Science* **2004**, *303*, 76−79. (c) Hänzelmann, P.; Schindelin, H. *Proc. Natl. Acad. Sci. U. S. A.* **2004**, *101*, 12870−12875. (d) Walsby, C. J.; Ortillo, D.; Yang, J.; Nnyepi, M. R.; Broderick, W. E.; Hoffman, B. M.; Broderick, J. B. *Inorg. Chem.* **2005**, *44*, 727−741. (e) Lepore, B. W.; Ruzicka, F. J.; Frey, P. A.; Ringe, D. *Proc. Natl. Acad. Sci. U. S. A.* **2005**, *102*, 13819−13824. (f) Vey, J. L.; Yang, J.; Li, M.; Broderick, W. E.; Broderick, J. B.; Drennan, C. L. *Proc. Natl. Acad. Sci. U. S. A.* **2008**, *105*, 16137−16141. (g) Yan, F.; LaMarre, J. M.; Röhrich, R.; Wiesner, J.; Jomaa, H.; Mankin, A. S.; Fujimori, D. G. *J. Am. Chem. Soc.* **2010**, *132*, 3953−3964. (h) Vey, J. L.; Drennan, C. L. *Chem. Rev.* **2011**, *111*, 2487−2506.

(8) (a) Johnson, R. W.; Holm, R. H. *J. Am. Chem. Soc.* **1978**, *100*, 5338−5344. (b) Evans, D. J. *Inorg. Chim. Acta* **1993**, *203*, 253−256. (c) Fu, Y.-J.; Yang, X.; Wang, X.-B.; Wang, L.-S. *Inorg. Chem.* **2004**, *43*, 3647−3655.

(9) Weigel, J. A.; Holm, R. H. *J. Am. Chem. Soc.* **1991**, *113*, 4184−4191.

(10) van Strijdonck, G. P. F.; ten Have, P. T. J. H.; Feiters, M. C.; van der Linden, J. G. M.; Steggerda, J. J.; Nolte, R. J. M. *Chem. Ber./Recl.* **1997**, *130*, 1151−1157.

(11) Terada, T.; Wakimoto, T.; Nakamura, T.; Hirabayashi, K.; Tanaka, K.; Li, J.; Matsumoto, T.; Tatsumi, K. *Chem. Asian J.* **2012**, *7*, 920−929.

(12) While the structures of **3**, **6**, and **8** were also analyzed by X-ray crystallography, the structural details are not discussed due to the insufficient quality of the crystals. The structures are shown in the Supporting Information, and the crystallographic data were deposited with the CCDC.

(13) Nag, S.; Banerjee, K.; Datta, D. *New J. Chem.* **2007**, *31*, 832−834.

(14) (a) Ménage, S.; Que, L., Jr. *Inorg. Chem.* **1990**, *29*, 4293−4297. (b) Hagadorn, J. R.; Que, L., Jr.; Tolman, W. B. *Inorg. Chem.* **2000**, *39*, 6086−6090. (c) Lee, D.; Lippard, S. J. *Inorg. Chim. Acta* **2002**, *341*, 1−11.

(15) A similar intermolecular hydrogen bonding interaction for zinc pyrrole-2-carboxylate was reported, see: Zevaco, T. A.; Görls, H.; Dinjus, E. *Polyhedron* **1998**, *17*, 2199−2206.

(16) Ohki, Y.; Tanifuji, K.; Yamada, N.; Imada, M.; Tajima, T.; Tatsumi, K. *Proc. Natl. Acad. Sci. U. S. A.* **2011**, *108*, 12635−12640.
(17) CV charts of **3**, **6**, and **9** are shown in the Supporting Information.
(18) Zhou, C.; Holm, R. H. *Inorg. Chem.* **1997**, *36*, 4066−4077.
(19) van Strijdonck, G. P. F.; van Haare, J. A. E. H.; van der Linden, J. G. M.; Steggerda, J. J.; Nolte, R. J. M. *Inorg. Chem.* **1994**, *33*, 999−1000.
(20) Holm et al. reported that the redox potentials of [4Fe−4S] clusters having a tridentate ligand and a neutral ligand such as imidazole, pyridine, or phosphine show a ca. 20 mV positive shift relative to the value of the acetate cluster, see ref 18.
(21) Ohno, R.; Ueyama, N.; Nakamura, A. *Inorg. Chem.* **1991**, *30*, 4887−4891.
(22) The theoretical analysis showed that the redox potential $[4Fe−4S]^{2+/+}$ of four cysteine coordinated [4Fe−4S] clusters is more positive than that of one aspartate and three cysteine coordinated [4Fe−4S] cluster in DMF, which is different from the results of our models, see: Takano, Y.; Yonezawa, Y.; Fujita, Y.; Kurisu, G.; Nakamura, H. *Chem. Phys. Lett.* **2011**, *503*, 296−300.
(23) The theoretical study showed similar results, see: Jensen, K. P.; Ooi, B.-L.; Christensen, H. E. M. *Inorg. Chem.* **2007**, *46*, 8710−8716.